

Insights Into the Pathogenesis of Catecholaminergic Polymorphic Ventricular Tachycardia From Engineered Human Heart Tissue

BACKGROUND: Modeling of human arrhythmias with induced pluripotent stem cell–derived cardiomyocytes has focused on single-cell phenotypes. However, arrhythmias are the emergent properties of cells assembled into tissues, and the impact of inherited arrhythmia mutations on tissue-level properties of human heart tissue has not been reported.

METHODS: Here, we report an optogenetically based, human engineered tissue model of catecholaminergic polymorphic ventricular tachycardia (CPVT), an inherited arrhythmia caused by mutation of the cardiac ryanodine channel and triggered by exercise. We developed a human induced pluripotent stem cell–derived cardiomyocyte–based platform to study the tissue-level properties of engineered human myocardium. We investigated pathogenic mechanisms in CPVT by combining this novel platform with genome editing.

RESULTS: In our model, CPVT tissues were vulnerable to developing reentrant rhythms when stimulated by rapid pacing and catecholamine, recapitulating hallmark features of the disease. These conditions elevated diastolic Ca^{2+} levels and increased temporal and spatial dispersion of Ca^{2+} wave speed, creating a vulnerable arrhythmia substrate. Using Cas9 genome editing, we pinpointed a single catecholamine-driven phosphorylation event, ryanodine receptor–serine 2814 phosphorylation by Ca^{2+} /calmodulin-dependent protein kinase II, that is required to unmask the arrhythmic potential of CPVT tissues.

CONCLUSIONS: Our study illuminates the molecular and cellular pathogenesis of CPVT and reveals a critical role of calmodulin-dependent protein kinase II–dependent reentry in the tissue-scale mechanism of this disease. We anticipate that this approach will be useful for modeling other inherited and acquired cardiac arrhythmias.

Sung-Jin Park, PhD*
Donghui Zhang, PhD*
Yan Qi, BS
Yifei Li, MD
Keel Yong Lee, PhD
Vassilios J. Bezzerides, MD, PhD
Pengcheng Yang, BS
Shutao Xia, BS
Sean L. Kim, BS
Xujie Liu, PhD
Fujian Lu, PhD
Francesco S. Pasqualini, PhD
Patrick H. Campbell, PhD
Judith Geva, MSW
Amy E. Roberts, MD
Andre G. Kleber, MD
Dominic J. Abrams, MD, MBA
William T. Pu, MD;
Kevin Kit Parker, PhD

*Drs Park and Zhang contributed equally.

Key Words: arrhythmias, cardiac biological engineering ■ CaMKII ■ catecholaminergic polymorphic ventricular tachycardia disease models ■ gene editing ■ stem cells

Sources of Funding, see page 402

© 2019 American Heart Association, Inc.

<https://www.ahajournals.org/journal/circ>

Clinical Perspective

What Is New?

- Engineered heart tissue fabricated from human pluripotent stem cell–derived cardiomyocytes effectively modeled catecholaminergic polymorphic ventricular tachycardia (CPVT) caused by dominant mutations in the cardiac ryanodine receptor (RYR2), including induction of arrhythmias by conditions that simulate exercise.
- Using selective pharmacology and genome editing, we identified activation of Ca²⁺/calmodulin-dependent protein kinase II and calmodulin-dependent protein kinase II–mediated phosphorylation of RYR2 at serine 2814 as critical events required to unmask the latent arrhythmic potential of CPVT-causing RYR2 mutations, highlighting a molecular pathway that links β-adrenergic stimulation to arrhythmogenesis in this disease.

What Are the Clinical Implications?

- This study identifies calmodulin-dependent protein kinase II activation as a central event in the triggering of arrhythmias in patients with CPVT, suggesting that calmodulin-dependent protein kinase II inhibition will be an effective and translatable strategy to treat CPVT caused by RYR2 mutations.
- Under exercise conditions, CPVT mutations create heterogeneities in cardiac impulse propagation that make the working myocardium vulnerable to reentrant arrhythmias initiated by triggered beats emanating from the His-Purkinje system.
- The human engineered heart tissue platform will be useful to dissect mechanisms and treatment responses in diverse forms of arrhythmia.

Catecholaminergic polymorphic ventricular tachycardia (CPVT) is an inherited arrhythmia caused predominantly by autosomal dominant mutation of the gene encoding the cardiac ryanodine receptor (RYR2), the main intracellular calcium release channel of cardiomyocytes.¹ Typically, patients with CPVT are asymptomatic at rest but develop potentially lethal ventricular tachycardia during exercise or emotional distress (Figure 1A and Figure 1A in the online-only Data Supplement). In wild-type (WT) cells, when the cardiac action potential opens the voltage sensitive L-type Ca²⁺ channel located in the plasma membrane, the resulting local influx of Ca²⁺ triggers release of Ca²⁺ from the sarcoplasmic reticulum via RYR2 (Figure 1B). The resulting increase in cytoplasmic Ca²⁺ leads to sarcomere contraction. As the cell enters diastole, RYR2 closes and cytosolic Ca²⁺ is pumped back into the sarcoplasmic reticulum. In cells carrying CPVT mutations, RYR2 releases more Ca²⁺ into the cytoplasm, resulting in elevated diastolic Ca²⁺, which drives exchange of sodium and calcium through the plasma membrane via

the sodium-calcium exchanger,³ leading to afterdepolarizations that may trigger additional action potentials. The molecular mechanism by which catecholamine stimulation unmasks the arrhythmic nature of CPVT mutations is not known, although catecholamine-induced activation of Ca²⁺-calmodulin–dependent protein kinase II (CaMKII) has been implicated.^{4,5} The mechanisms by which RYR2 mutation and consequent cellular abnormalities such as afterdepolarizations cause the organ-level phenotype of ventricular tachycardia are also uncertain. One theory is that triggered activity in the His-Purkinje system initiates ventricular tachycardia.^{6,7} However, in a mouse CPVT model, ventricular arrhythmias required the CPVT-causing mutation in working myocardium, in addition to the His-Purkinje system,⁸ suggesting that CPVT-causing mutations produce a substrate for reentrant or focal arrhythmias in the working myocardium. Understanding how single-cell Ca²⁺ handling abnormalities lead to tissue, organ, and clinical manifestations of CPVT has been hampered by limitations of currently available disease models.

The advent of induced pluripotent stem cell (iPSC) technology and efficient methods to differentiate iPSCs to cardiomyocytes (iPSC-CMs) has created exciting opportunities to study inherited arrhythmias.⁹ iPSC-CMs have been generated from patients with CPVT^{5,10–13} and other inherited arrhythmias and have been shown to capture key features of these diseases, including abnormal action potential duration and drug responses.⁹ However, current iPSC-CM models of arrhythmia have been limited to isolated cells or cell clusters, leaving a large gap in modeling clinical arrhythmias, which are the emergent properties of cells assembled into myocardial tissue.¹⁴

We^{15–17} and others¹⁸ have developed engineered cardiac microphysiological systems that induce stem cell–derived and primary cardiomyocytes to adopt native-like laminar tissue architecture, permitting tissue-level measurement of contractility. Here, we integrated an engineered cardiac tissue with optogenetics, optical mapping, and iPSC-CMs to create a human tissue model of CPVT. We used this model and Cas9-mediated genome editing to investigate the molecular and cellular mechanisms underlying exercise-induced ventricular tachycardia in this disease.

METHODS

The expanded Methods section in the online-only Data Supplement provides a full description of experimental procedures. The authors declare that all supporting data are available within the article and its online-only Data Supplement. Materials will be shared on reasonable request.

Human iPSCs and Differentiation of iPSC-CMs

Patients provided informed consent to participate in this study under protocols approved by the Boston Children's Hospital Institutional Review Board. Fibroblasts were cultured from

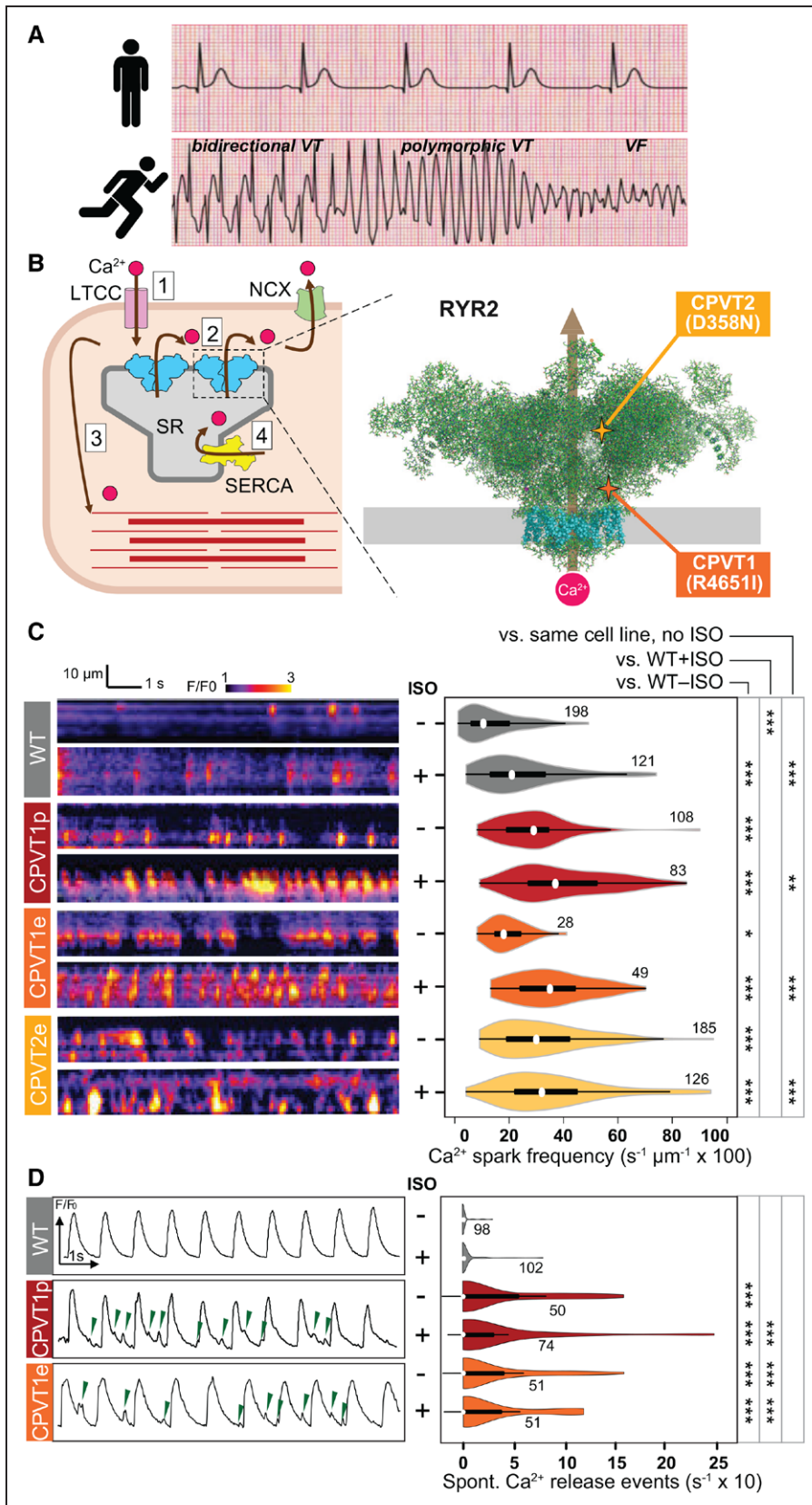


Figure 1. Characterization of Ca²⁺ oscillations in induced pluripotent cell-derived cardiomyocyte (iPSC-CM) clusters.
A, Patients with catecholaminergic polymorphic ventricular tachycardia (CPVT) have normal resting ECGs but severe, potentially life-threatening arrhythmias with exercise. Traces are idealized sketches shown for illustration purposes. **B**, CPVT pathophysiology. **Left**, Cartoon of cardiomyocyte Ca²⁺-induced Ca²⁺ release. (1) Action potential opens L-type Ca²⁺ channel (LTCC). (2) Ca²⁺ induces opening of ryanodine receptor (RYR2) and release of Ca²⁺ from the sarcoplasmic reticulum (SR). (Continued)

Downloaded from <http://ahajournals.org> by on August 22, 2019

Figure 1 Continued. (3) Elevated intracellular Ca^{2+} induces myofilament contraction. (4) Ca^{2+} is cleared from the cytosol by sarcoplasmic/endoplasmic reticulum calcium ATPase (SERCA) and sodium-calcium exchanger (NCX). **Right**, CPVT mutations in RYR2 increase diastolic Ca^{2+} leak. Cartoon shows RYR2 structure based on CryoEM data.² Gray rectangle indicates the SR membrane. Transmembrane domains are shown in cyan. CPVT-causing RYR2 mutations in this study are highlighted. **C**, Incidence of Ca^{2+} sparks in quiescent iPSC-CMs. **Left**, Representative confocal line scans of Fluo-4 signal within individual iPSC-CMs in cell clusters. **Right**, Quantitative analysis. Number by each shape denotes number of cells examined. **D**, Incidence of spontaneous Ca^{2+} release events in spontaneously beating iPSC-CMs. **Left**, Representative Ca^{2+} signal traces, spatially averaged over confocal line scans within individual iPSC-CMs in cell clusters. Green arrowheads indicate spontaneous Ca^{2+} release events. **Right**, Quantitative analysis. Number by each shape denotes number of cells examined. Steel-Dwass nonparametric test with multiple-testing correction. ISO indicates isoproterenol; VF, ventricular fibrillation; VT, ventricular tachycardia; and WT, wild-type. * $P < 0.05$, ** $P < 0.01$, *** $P < 0.001$.

skin biopsies and reprogrammed by episomal transfection with reprogramming factors. iPSC lines were maintained in mTeSR1 medium (STEMCELL Technologies) and passaged in versene solution (15040066, Thermo Fisher Scientific) every 5 days on culture dishes precoated with Matrigel (hESC-Qualified Matrix, LDEV-Free, Corning) diluted 1:100.

The procedures for clustered regularly interspaced short palindromic repeat/Cas9 genome editing using a WT PGP1 human iPSC line containing doxycycline-inducible Cas9 were described in detail in a recent publication.¹⁹ Guide RNA and homology-directed repair constructs are provided in the [Methods in the online-only Data Supplement](#). We predicted Cas9-gRNA off-target sites using <http://crispr.mit.edu/>.²⁰ Amplicons containing the top 10 predicted sites were amplified from iPSCs and Sanger sequenced.

iPSCs differentiated to cardiomyocytes by modulating WNT signaling with CHIR99021 and IWR-1. iPSC-CMs were enriched by culture in lactate-containing media. Commercial human iPSC-derived cardiomyocytes (Cor4U; Axiogenesis, Cologne, Germany) were cultured according to the manufacturer's instructions.

Opto-Muscular Thin Film Construction

Micromolded gelatin was fabricated on glass coverslips such that the gelatin in the base region of muscular thin films (MTFs) would firmly attach to the glass coverslips but the gelatin in the cantilever region could be easily peeled. Cantilevers (1 mm wide \times 2 mm long) were laser engraved into the dehydrated micromolded gelatin. Gelatin chips were treated with ultraviolet-ozone for 90 seconds and rehydrated in a 2-mmol/L MES (2-(N-morpholino)ethanesulfonic acid) solution, pH 4.5, with 1 mg/ml collagen and 0.1 mg/mg fibronectin. After 2 hours at room temperature, the collagen and fibronectin solution was replaced with PBS. The gelatin chips were stored at 4°C until cell seeding.

Dissociated iPSC-CMs were plated on gelatin chips and then transduced with channelrhodopsin (ChR2) lentiviral vector, in which the cardiac troponin T promoter that drives ChR2-eYFP was constructed on the basis of the FCK(1.3) GW plasmid with the cardiac troponin T promoter ChR2 and enhanced yellow fluorescent tag.^{21,22}

Calcium Imaging of Cell Clusters

iPSC-CMs were seeded on Matrigel-coated glass bottom dishes for 5 days. After loading with Fluo-4 (F14201, Thermo Fisher Scientific) or Fluo-4 (F14201, Thermo Fisher Scientific), cells were imaged with an Olympus FV1000 using line-scan mode (10 milliseconds per line, 1000 lines per recording). When indicated, cells were treated with protein kinase A (PKA) inhibitor (myristoylated 14-22 amide, 1 $\mu\text{mol/L}$) or CaMKII inhibitor (myristoylated autocalmitide-2-related inhibitory peptide [AIP]). Isoproterenol and dantrolene were each used at 1 $\mu\text{mol/L}$.

Optical Recording of Opto-MTFs

Opto-MTFs were imaged using a modified tandem-lens microscope (Scimedia) for simultaneous Ca^{2+} imaging and contractility measurement with optogenetic stimulation ([Figure II in the online-only Data Supplement](#)). Optogenetic stimulation was delivered with optical fibers mounted 500 μm above the gelatin chips.

Three days after transduction with ChR2 lentivirus, opto-MTFs were loaded with X-Rhod-1. Culture media was replaced with Tyrode solution and maintained at 37°C. When indicated, opto-MTFs were treated with 6 $\mu\text{mol/L}$ dantrolene or 2 $\mu\text{mol/L}$ AIP.

Opto-MTFs were stimulated with 10-millisecond optical pulses over a range of frequencies from 0.7 to 3 Hz with a custom LabVIEW program (National Instruments). For each recording, Ca^{2+} and dark field images were simultaneously acquired with 2000 and 400 frames at a frame rate of 200 and 100 Hz over 10 and 4 seconds, respectively.

Postprocessing of the raw calcium and dark-field imaging data was conducted with custom software written in MATLAB (MathWorks).

Statistical Analysis

Statistical analysis was performed with JMP Pro 14 (SAS Institute, Inc).

The significance between groups from cell cluster measurements was evaluated with the Steel-Dwass nonparametric test with multiple-testing correction. Statistical analysis of Western blots was performed with the Tukey-Kramer honestly significant difference test for multiple groups or Student *t* test for 2 groups.

For tissue-level differences, between-group differences in occurrence of reentry were evaluated with the Pearson χ^2 test and the Bonferroni correction for multiple comparisons with corrected *P* values by dividing *P* values by number of possible pairwise comparison tests (ie, 0.05/6, 0.01/6, 0.001/6 for 4 different tissues and 6 possible pairwise comparison tests; 0.05/3, 0.01/3, 0.001/3 for 3 different tissues and 3 possible pairwise comparison tests). Heterogeneities of calcium handling in the iPSC-CMs used in this study and neonatal rat ventricular myocytes or commercial iPSC-CMs were compared with 1-way ANOVA followed by the Tukey-Kramer honestly significant difference test. Tissue-level functional differences were tested with the Student *t* test corrected with Benjamini-Hochberg multiple-testing correction (false discovery rate, 20%).²³

RESULTS

Ca^{2+} Handling in Individual iPSC-CM Within a Cell Cluster

We obtained skin fibroblasts from a patient with CPVT. This patient had a normal resting ECG but exercise-in-

duced bidirectional and polymorphic ventricular tachycardia (Figure 1A in the online-only Data Supplement). Genotyping revealed that the patient had a heterozygous point mutation in RYR2 that caused substitution of isoleucine for arginine at position 4651 (R4651I; Figure 1B and Figure 1B and 1C in the online-only Data Supplement). Clinical genotyping did not implicate other candidate inherited arrhythmia genes. The fibroblasts were reprogrammed into iPSCs (line CPVT1p, where p indicates patient-derived; Figure 1C). We used Cas9 genome editing¹⁹ to introduce the patient mutation into a WT iPSC line, PGP1, yielding a CPVT line (PGP1-RYR2R4651I, abbreviated CPVT1e, where e denotes engineered) otherwise isogenic to WT (Figure 1B and 1D in the online-only Data Supplement). In addition, we similarly used Cas9 genome editing to introduce a second CPVT-causing mutation, substitution of asparagine for aspartate at position 358 (D358N) into PGP1, yielding a second engineered CPVT line (PGP1-RYR2D358N, abbreviated CPVT2e; Figure 1B and Figure 1B and 1I in the online-only Data Supplement). Sequencing of the top 10 predicted off-target genome editing sites for CPVT1e and CPVT2e did not identify unintended genome modification (Figure 1V in the online-only Data Supplement). These iPSCs had normal karyotype and robustly differentiated into iPSC-CMs with comparable efficiency (Figure 1V in the online-only Data Supplement).

We analyzed Ca²⁺ handling of WT, CPVT1p, CPVT1e, and CPVT2e iPSC-CMs by loading spontaneously beating iPSC-CM clusters (3–10 cells per cluster) with the Ca²⁺-sensitive dye Fluo-4 and performing confocal line-scan imaging within individual cells of a cluster. These clusters exhibited periods of spontaneous rhythmic beating interspersed with periods of quiescence. When recorded during periods of quiescence, both patient-derived and genome-edited isogenic CPVT1 iPSC-CMs had more frequent Ca²⁺ sparks than WT,²⁴ and this was further exacerbated by isoproterenol, a β -sympathomimetic (Figure 1C). The genome-edited isogenic CPVT2 iPSC-CM line also had more frequent Ca²⁺ sparks than WT, although this was not further exacerbated by isoproterenol (Figure 1C). During spontaneous beating, we observed spontaneous Ca²⁺ release events interspersed between Ca²⁺ transients (Figure 1D, left). Quantitative analysis showed greater frequency of spontaneous Ca²⁺ release events in beating CPVT iPSC-CMs, with and without isoproterenol stimulation (Figure 1D, right). These spontaneous Ca²⁺ release events correlated with membrane depolarization (Figure 1VH–1VJ in the online-only Data Supplement), consistent with afterdepolarizations previously reported in CPVT iPSC-CMs and CMs.^{4,5,12} These results confirm that both CPVT mutations tested are sufficient to increase Ca²⁺ release from RYR2, consistent with Ca²⁺ handling abnormalities reported in iPSC-CMs with other CPVT-causing RYR2 mutations.^{5,10–13}

Opto-MTF–Engineered Heart Tissue Model of Inherited Arrhythmia

Because clinical arrhythmias emerge from the collective behavior of cardiomyocytes assembled into tissues, to better model inherited arrhythmias we integrated muscular thin films (MTFs),²⁵ optogenetics, and optical mapping to yield opto-MTFs, a platform that permits simultaneous assessment of myocardial Ca²⁺ transient propagation and contraction (Figure 2A and Figures 2I and 2J in the online-only Data Supplement). iPSC-CMs were seeded onto 10×10-mm micromolded gelatin MTFs¹⁶ (Figure 2I in the online-only Data Supplement), so that they assembled into tissue with parallel cell alignment characteristic of native myocardium (Figure 2I and Movie 1 in the online-only Data Supplement). Lentivirus was used to program iPSC-CMs to express ChR2, a light-gated channel that allows cardiomyocytes to be paced with 488-nm light, as described previously.^{25,26} ChR2 expression in cardiomyocytes was shown previously to alter minimally the electrophysiological properties of the tissue.²¹ Using 10-millisecond pulses of 488-nm light, we optically stimulated an ≈ 0.79 -mm² region, containing ≈ 500 cells, at 1 end of the opto-MTFs. This local activation stimulated Ca²⁺ transient propagation across the opto-MTFs in the direction of the long axis of muscle fibers. Propagation of Ca²⁺ transients was recorded with the Ca²⁺ sensitive fluorescent dye X-Rhod-1 at a resolution of 100×100 μ m (Figure 2C and 2D and Figure 2J and Movies 2 and 3 in the online-only Data Supplement). Ca²⁺ transient propagation into 2 film cantilevers at the far end of the opto-MTF induced iPSC-CM contraction, curving the cantilever and permitting measurement of mechanical systole (Figure 2C and 2D and Figure 2J and Movies 2 and 3 in the online-only Data Supplement).^{15–17} Each chip was composed of 3 individual MTFs (3×10 mm) that were isolated from one another, permitting independent assays within the same chip (Figure 2K and Movies 4 and 5 in the online-only Data Supplement). Spatiotemporal characteristics of the opto-MTFs, including propagating Ca²⁺ transient activation time and propagation speed (CaS) and direction, were measured from the Ca²⁺ imaging data (Figure 2E). At a pacing rate of 1.5 Hz, the heterogeneity in CaS across space and time observed for the iPSC-CMs used in this study was comparable to or less than that observed with neonatal rat ventricular myocytes or commercial human stem cell–derived cardiomyocytes (Figure 2E and Figure 2L in the online-only Data Supplement).

We used the opto-MTF platform to characterize the properties of CPVT iPSC-CMs assembled into engineered heart tissues. The spontaneous beating frequency of CPVT tissues was not different from that of WT tissues (Figure 2M in the online-only Data Supplement). Spontaneous beats in both WT and CPVT originated

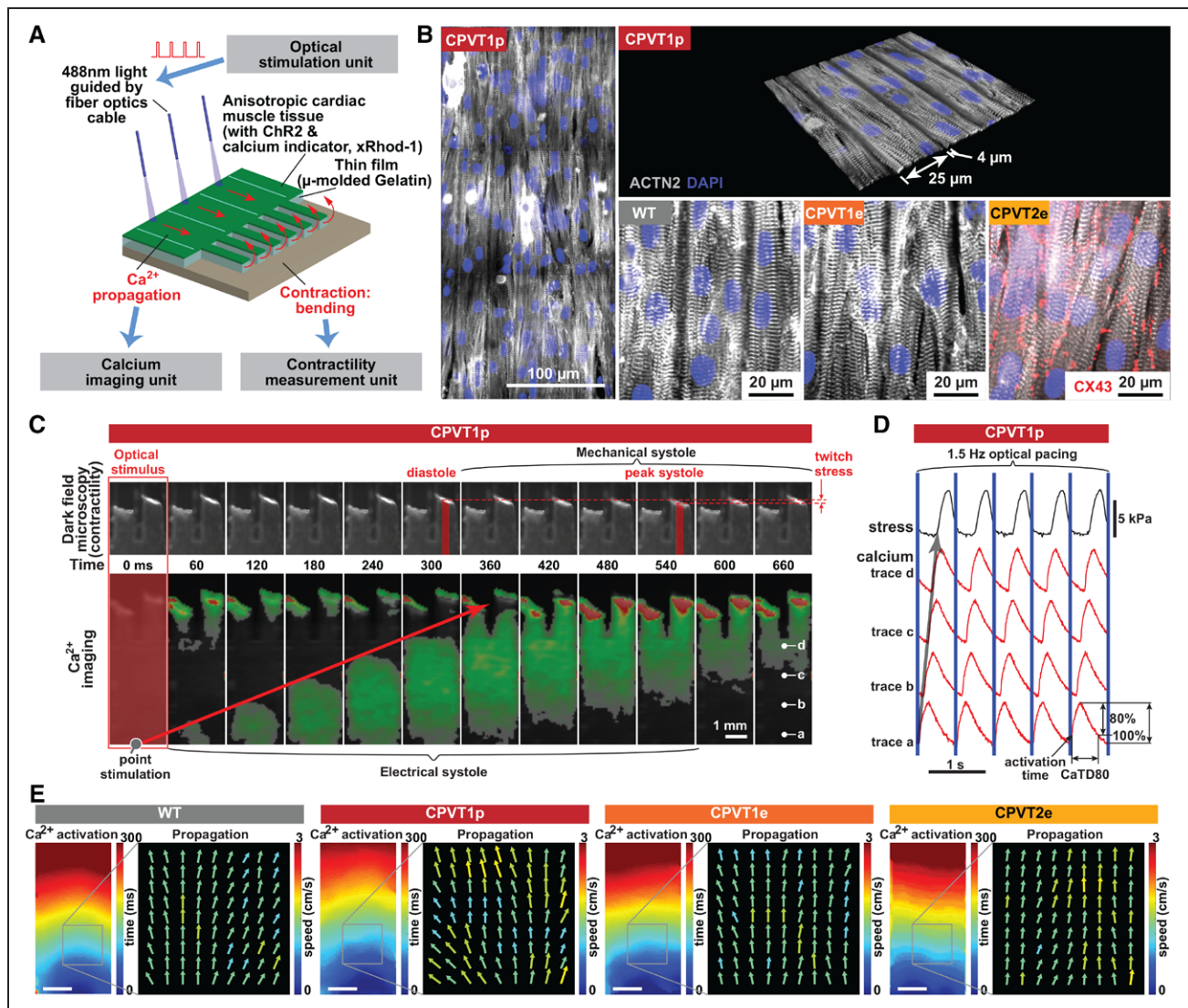


Figure 2. Opto-muscular thin film (MTF)-engineered heart tissue for arrhythmia modeling.

A, Schematic of opto-MTF system to optically pace and optically measure tissue-level Ca^{2+} wave propagation and contraction. Cardiomyocytes programmed to express channelrhodopsin (ChR2) are seeded onto micromolded gelatin with flexible cantilevers on 1 end. Focal illumination with optical fibers excites cells, resulting in Ca^{2+} wave propagation along the MTF and into the cantilevers. Ca^{2+} wave propagation is measured by fluorescent imaging of the Ca^{2+} -sensitive dye X-Rhod-1; mechanical contraction is assessed by dark-field imaging of the cantilevers. **B**, Confocal images of ACTN2-stained opto-MTFs. Micromolded gelatin induces induced pluripotent cell-derived cardiomyocytes to grow with their long axis aligned with the long axis of the MTF. **C**, Excitation-contraction coupling in CPVT1p opto-MTFs. Representative time-lapse images show Ca^{2+} wave propagation and mechanical systole recorded induced by optogenetic point stimulation. **D**, Ca^{2+} traces recorded at the points labeled a through d in the **right-most** image of **C**. Blue lines indicate optical pacing at the stimulation point. Activation time is the time to the maximal Ca^{2+} signal upstroke velocity. CaTD80 is the duration of the Ca^{2+} transient at 80% decay. **E**, Spatial maps of activation time and Ca^{2+} wave speed and direction for WT, CPVT1p, CPVT1e, and CPVT2e opto-MTFs at 1.5 Hz pacing, demonstrating well-ordered tissue behavior under these conditions. Bar, 1 mm. CPVT indicates catecholaminergic polymorphic ventricular tachycardia; and WT, wild-type.

from tissue edges, as expected from reduced source-to-load mismatch present at these sites. Whereas spontaneously beating, unstimulated CPVT iPSC-CMs in cell clusters composed of a few cells often exhibited Ca^{2+} transients with aberrant waveforms (Figure 1D), we did not observe any abnormal Ca^{2+} traces in spontaneously beating CPVT or control tissues recorded at lower resolution (Figure XB–XE in the online-only Data Supplement). These data indicate that Ca^{2+} transient abnormalities observed in single cells do not coordinate in spontaneously beating tissues to yield detectable abnormalities in tissue-level propagating Ca^{2+} transients

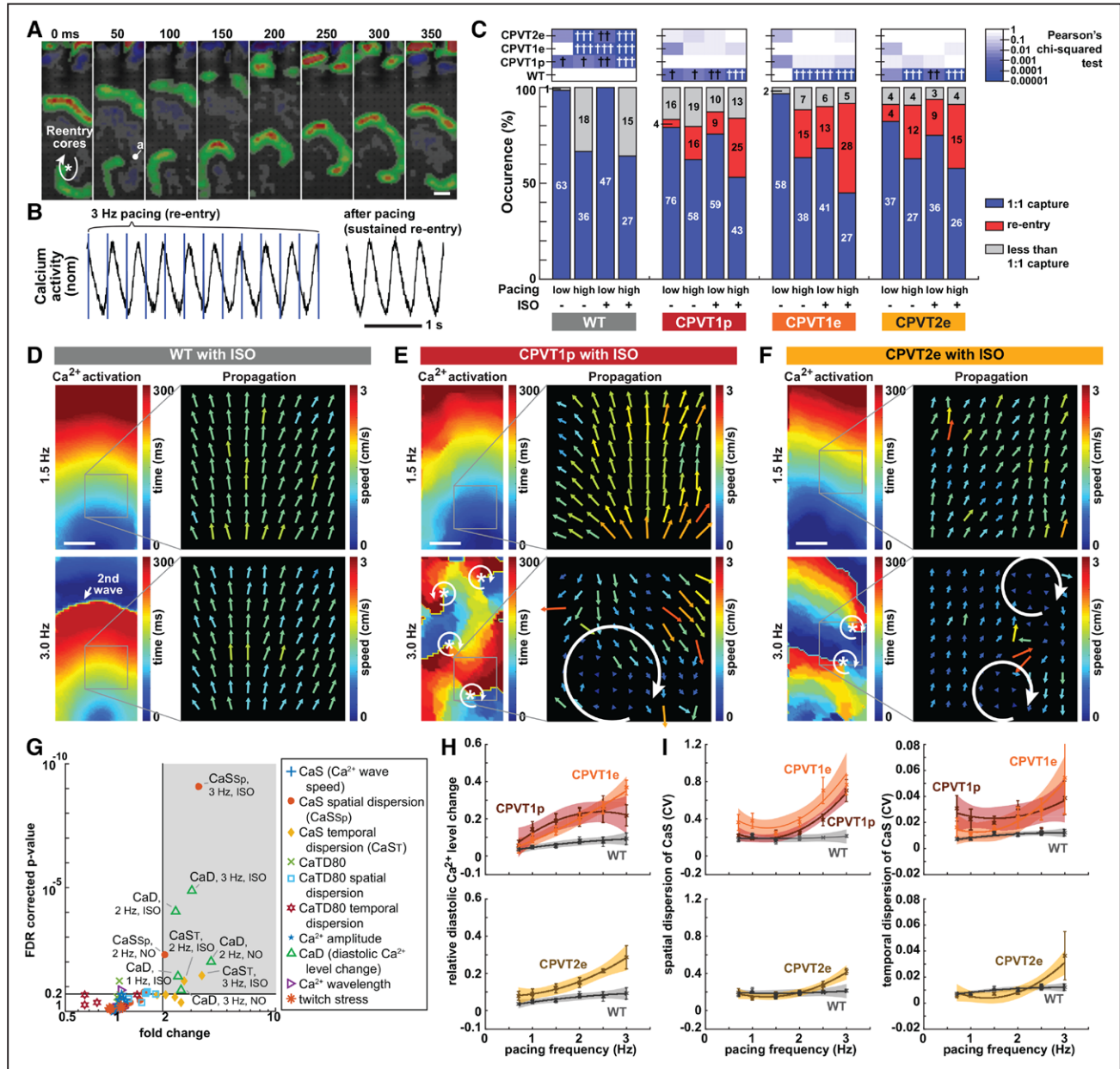
(referred to hereafter in this study as calcium waves). This quiescent baseline behavior of spontaneously beating CPVT tissues parallels the normal baseline phenotype of patients with CPVT, who have few arrhythmias in the absence of exercise or emotional stress.

High Pacing Rate and β -Adrenergic Stimulation Induce Reentry in CPVT Opto-MTFs

Patients with CPVT are at risk for developing ventricular tachycardia during exercise or emotional stress. To

simulate key features of these provocative conditions in vitro, we treated opto-MTFs with increasing optical pacing frequency (1–3 Hz) or β -adrenergic stimulation (0–10 μ mol/L isoproterenol). Remarkably, the 3 CPVT iP-SC-CM lines but not WT opto-MTFs were vulnerable to

spiral wave reentry, a cause of tachycardia at the tissue level (Figure 3A and 3B and [Movies VI–IX in the online-only Data Supplement](#)). The combination of both high pacing rate and isoproterenol most potently evoked reentry (Figure 3C). During reentry, the opto-MTF canti-



levers generated less stress and induced asynchronous contraction (Figure XI and Movies VI, VII, and X in the online-only Data Supplement), mimicking the loss of forceful coordinated contraction that impairs cardiac output in clinical ventricular tachycardia. Dantrolene, a small molecule that inhibits release of Ca^{2+} through ryanodine receptors, inhibits CPVT arrhythmias.^{27,28} Consistent with previous studies,^{10,27} dantrolene reduced abnormal Ca^{2+} handling in CPVT iPSC-CMs (Figure XII in the online-only Data Supplement). Dantrolene likewise suppressed reentry in CPVT1e opto-MTFs (Figure XIII in the online-only Data Supplement). These data show that assembly of CPVT iPSC-CMs into opto-MTFs models key features of the disease at a tissue level. Furthermore, the data implicate reentry as an arrhythmia mechanism in CPVT.

To better understand the development of reentry in CPVT tissues, we analyzed optical mapping data of Ca^{2+} wave propagation. When challenged with 3-Hz pacing and isoproterenol, WT opto-MTFs retained organized Ca^{2+} waves, as shown by coherent Ca^{2+} activation maps and relatively homogeneous Ca^{2+} wave propagation speed and direction (Figure 3D). At 1.5-Hz pacing with or without isoproterenol, CPVT1p, CPVT1e, and CPVT2e opto-MTFs also were relatively coordinated (Figure 3E and 3F, top). However, rapid pacing of the same CPVT tissues induced reentry in which Ca^{2+} waves propagated in a circular pattern, associated with increased spatial dispersion of CaS (Figure 3E and 3F, bottom, and Figure XIV and Movie XI in the online-only Data Supplement).

To characterize the tissue-level mechanisms that make CPVT tissues vulnerable to reentry, we compared WT with CPVT1 tissues for 10 different parameters (CaS, spatial and temporal dispersion of CaS, Ca^{2+} transient duration at 80% recovery, spatial and temporal dispersion of Ca^{2+} transient duration at 80% recovery, relative diastolic Ca^{2+} level change from basal condition, Ca^{2+} wave amplitude, Ca^{2+} wavelength, and twitch stress) at 3 different pacing rates (1, 2, and 3 Hz) with and without isoproterenol (Figure 3G and Figure XV in the online-only Data Supplement). For these analyses of the conditions that made CPVT1 tissues vulnerable reentry substrates, we focused on recordings with 1:1 capture and without active reentry. Under higher pacing rates and isoproterenol stimulation, CPVT1 tissues differed from WT (>2-fold change, nominal $P < 0.05$, and false discovery rate <0.2) in 3 parameters: relative diastolic Ca^{2+} level, spatial dispersion of CaS, and temporal dispersion of CaS. Specifically, significant differences were observed in relative diastolic Ca^{2+} level at 3 Hz+isoproterenol, 2 Hz+isoproterenol, and 1 Hz+isoproterenol; temporal dispersion of CaS at 3 Hz+isoproterenol and 2 Hz+isoproterenol; and spatial dispersion of CaS at 3 Hz+isoproterenol and 2 Hz–isoproterenol. We further analyzed the effect of

pacing rate on these 3 parameters in isoproterenol-stimulated CPVT and WT tissue (Figure 3H and 3I and Figure XV in the online-only Data Supplement). In isoproterenol-stimulated WT tissues, diastolic Ca^{2+} levels and spatial and temporal dispersion of CaS were relatively insensitive to changes in pacing rate from 1 to 3 Hz. In contrast, as CPVT1p, CPVT1e, and CPVT2e tissues were paced at higher rates, they developed greater relative diastolic Ca^{2+} level and greater spatial and temporal dispersion of CaS (Figure 3H and 3I and Figure XV in the online-only Data Supplement). Dispersion of CaS was also manifested by irregular Ca^{2+} activation maps observed in CPVT tissue paced at 3 Hz (Movie XI and Figure XIV in the online-only Data Supplement). These irregular Ca^{2+} activation maps were not observed when the same tissues were paced at 2 Hz (Movie XII and Figure XIV in the online-only Data Supplement). Because heterogeneity increases tissue vulnerability to reentry,¹⁴ this analysis indicates that rapid pacing and isoproterenol stimulation create a vulnerable arrhythmia substrate by increasing spatial and temporal heterogeneity in CaS. This increased tissue heterogeneity might be linked to pacing-dependent elevation of diastolic Ca^{2+} , which drives afterdepolarizations and impairs gap junction function,²⁹ thereby potentially reducing intercellular connectivity.

We next analyzed events that initiated reentry in the vulnerable CPVT substrate. We identified 8 recordings that captured the initiation of reentry (Table I in the online-only Data Supplement). The rare reentry events that we observed at low pacing rates (Figure 3C) were initiated by spontaneous Ca^{2+} waves originating from edges of the tissue that collided with pacing-driven Ca^{2+} waves (Movie X and Figure XVI in the online-only Data Supplement). High pacing rates suppressed these spontaneous Ca^{2+} waves, and reentry events were initiated by regional conduction block (Figure 4 and Movies XIII and XIV in the online-only Data Supplement). Isoproterenol-treated CPVT1p tissue paced at 2 Hz showed well-ordered Ca^{2+} wave propagation (Figure 4A and 4B). When the same tissue was paced at 3 Hz, there was greater dispersion of propagation velocity, including regions with functional conduction block (Figure 4C, gray areas in velocity vector field). Ca^{2+} waves propagating around the focal block reentered the original path, resulting in rotor formation. A similar example of reentry initiation with functional conduction block in CPVT1e and CPVT2e tissues is shown in Movies VIII, XV, and XVI and Figure XVII in the online-only Data Supplement. Although the mechanisms underlying functional, regional conduction block in CPVT tissue require further study, they were associated with elevated relative diastolic Ca^{2+} (Figure 3G and 3H), which could reduce iPSC-CM excitability³⁰ and cell-cell coupling.²⁹

Together, our engineered tissue model demonstrates that CPVT tissue is vulnerable to circus movement with

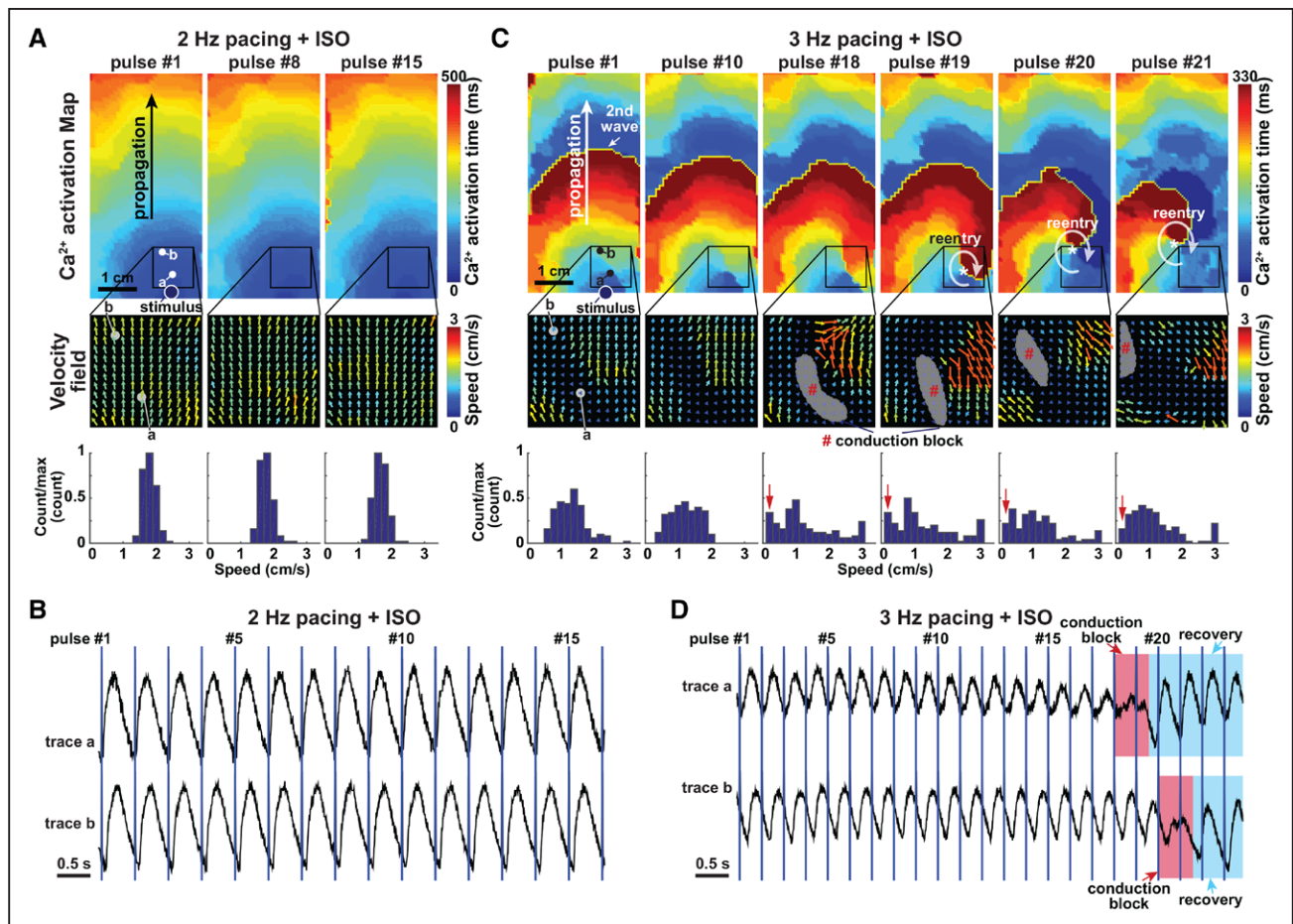


Figure 4. Initiation of reentry in catecholaminergic polymorphic ventricular tachycardia (CPVT) opto-muscular thin films (MTFs).

A, CPVT1p opto-MTF at 2-Hz pacing with isoproterenol (ISO). The Ca^{2+} activation map and velocity fields were well ordered. Speed histogram reflects narrow range of values. **B**, Ca^{2+} tracings from points a and b in **A**. **C**, The same opto-MTF as in **A** paced at 3 Hz with ISO. There are greater heterogeneity in the velocity field and disorganization of the Ca^{2+} activation map. Localized conduction block that permitted reentrant Ca^{2+} wave propagation becomes evident at pulses 18 and 19. Histograms indicate greater spatial dispersion of speed. **D**, Ca^{2+} tracings at points a and b in **C**. Red shading indicates conduction block overlying recording points; blue shading, recovery from block.

reentry. Rapid pacing and isoproterenol stimulation increased relative diastolic Ca^{2+} and spatiotemporal dispersion of Ca^{2+} . In this context, localized conduction block initiated rotor formation.

CaMKII Phosphorylation of RYR2–Serine 2814 Is Required to Unmask CPVT Arrhythmic Potential

Although catecholamine stimulation is well known to provoke arrhythmia in CPVT, the molecular targets through which β -adrenergic stimulation unmasks the latent arrhythmic potential of RYR2 mutations were incompletely defined. β -Adrenergic stimulation activates numerous signaling pathways, including CaMKII and PKA (Figure 5A). When we inhibited PKA using a potent, cell-permeable peptide,³¹ the incidence of Ca^{2+} sparks was not significantly reduced in CPVT1p iPSC-CMs (Figure 5B). In contrast, CaMKII inhibition with cell-permeable AIP (Figure XVIII A in the online-only Data Supplement), a highly selective and potent CaM-

KII inhibitor,³² strongly reduced the incidence of Ca^{2+} sparks and afterdepolarizations in CPVT1p, CPVT1e, and CPVT2e iPSC-CMs (Figure 5B and Figure XVIII B and XVIII C in the online-only Data Supplement). This effect is consistent with previous reports using a small-molecule inhibitor^{4,5} and with a recently reported CaMKII-dependent, PKA-independent pathway that mediates arrhythmogenesis provoked by adrenergic stimulation.³³ To model the effect of CaMKII inhibition at the tissue level, we treated CPVT1 and CPVT2 opto-MTFs with AIP. AIP inhibited the development of reentry provoked by rapid pacing and isoproterenol (Figure 5C and Movie XVII in the online-only Data Supplement). Analysis of diastolic Ca^{2+} level (Figure 5D) and spatial and temporal dispersion of Ca^{2+} wave speed (Figure 5E) showed that these key parameters of CPVT tissue vulnerability were normalized by AIP. These data suggest that CaMKII is a key signaling molecule in the pathogenesis of CPVT.

CaMKII targets multiple proteins that directly or indirectly affect Ca^{2+} handling.³⁴ One important CaMKII target is serine 2814 (S2814) on RYR2 itself³⁵ (Figure 5A).

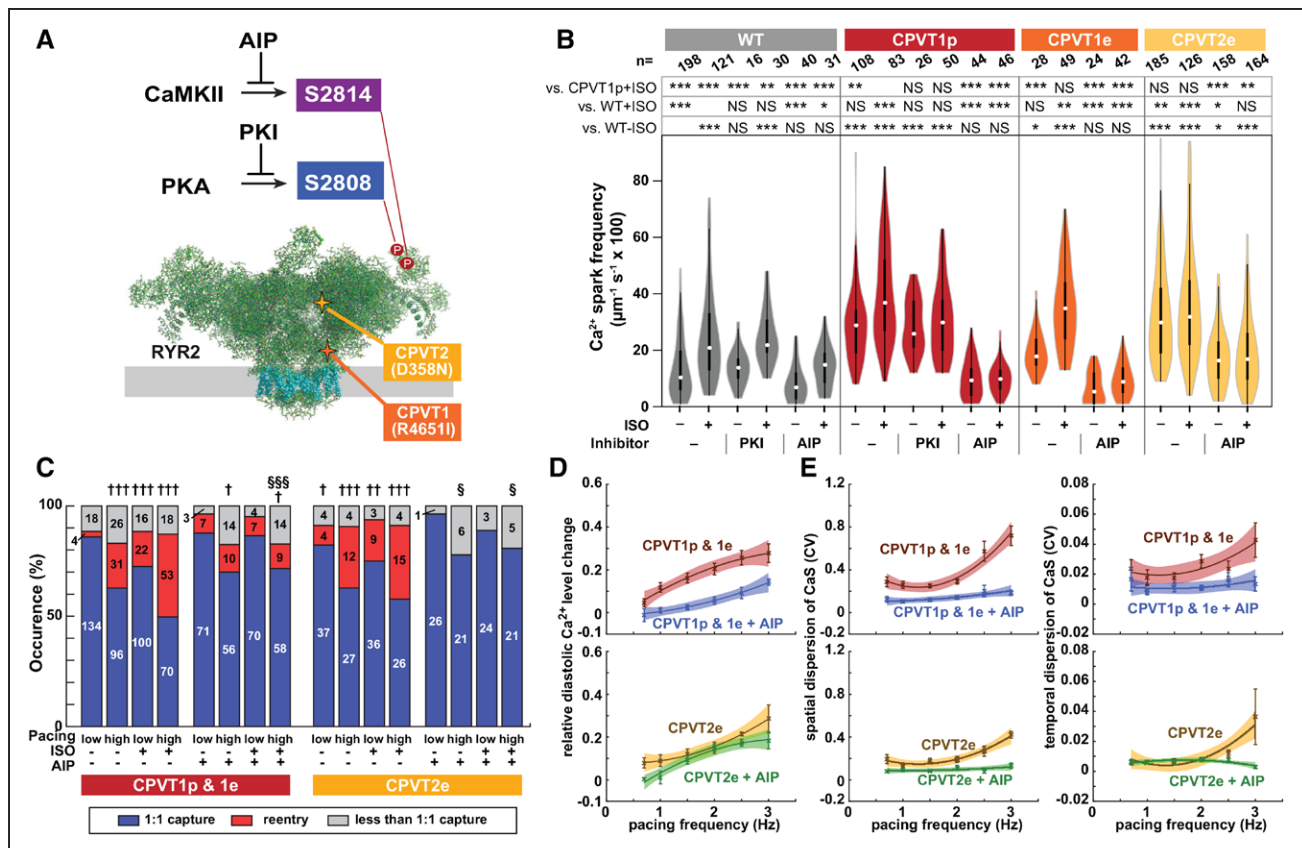


Figure 5. Ca²⁺-calmodulin-dependent protein kinase II (CaMKII) inhibition suppresses the catecholaminergic polymorphic ventricular tachycardia (CPVT) arrhythmic phenotype.

A, Schematic of ryanodine receptor (RYR2; 2 subunits of tetramer shown). Three key residues are highlighted: S2808, the target of protein kinase A (PKA) phosphorylation; serine 2814 (S2814), the target of CaMKII phosphorylation; and R46511, mutated in CPVTp. **B**, Induced pluripotent stem cell-derived cardiomyocytes (iPSC-CMs) in isolated cell clusters were treated with isoproterenol (ISO) and selective CaMKII (autocamide-2-related inhibitory peptide [AIP]) or PKA inhibitors (PKIs). Ca²⁺ sparks were imaged by confocal line scanning within individual iPSC-CMs. Data without inhibitors are the same as in Figure 1C. Steel-Dwass nonparametric test with multiple testing correction **P*<0.05, ***P*<0.001, ****P*<0.001. **C**, Occurrence of reentry in CPVT1 and CPVT2 engineered tissues treated with a CaMKII inhibitor (AIP). Bars are labeled with sample sizes. Pearson χ^2 test. †Versus wild-type (WT) with the same pacing and ISO conditions; §Versus CPVT with the same pacing and ISO conditions. The Bonferroni correction for multiple comparisons was applied for 3 possible pairwise tests performed with a corrected *P* threshold. †§*P*<0.05/3. ††*P*<0.01/3. †††§§§*P*<0.001/3. **D** and **E**, Relative diastolic Ca²⁺ level change from basal condition (**D**), and spatial and temporal dispersion of Ca²⁺ wave propagation speed (**E**) as a function of pacing frequency under ISO stimulation in CPVT1 and CPVT2 before and after AIP loading. Only tissues responding 1:1 to every stimulus were included in **D** and **E** (n=33 CPVT1p, 15 CPVT1p+AIP, 13 CPVT1e, 15 CPVT2e, and 9 CPVT2e+AIP from >3 harvests). NS indicates not significant.

RYR2-S2814 phosphorylation by CaMKII enhances diastolic RYR2 Ca²⁺ leak and is proarrhythmic.³⁶ To test the hypothesis that CaMKII-mediated phosphorylation of RYR2-S2814 is essential for expression of CPVT mutations, we used Cas9 genome editing to replace S2814 with alanine (S2814A) in RYR2 alleles in both RYR2 WT and RYR2^{R46511/+} backgrounds and showed that these mutations block this phosphorylation event (Figures IV and XIX in the online-only Data Supplement). We refer to these mutant alleles as WT-S2814A and CPVT1e-S2814A, respectively. RYR2 is also phosphorylated on S2808 by PKA,³⁷ and this phosphorylation event has been implicated in increasing RYR2 diastolic Ca²⁺ leak.³⁸ Therefore, we used genome editing to generate analogous RYR2-S2808A homozygous mutant lines, called WT-S2808A and CPVT1e-S2808A (Figures IV and XIX in the online-only Data Supplement). In keeping with the effect of CaMKII inhibitory peptide, in quiescent

iPSC-CMs in cell clusters, the incidence of Ca²⁺ sparks in CPVT1e-S2814A was less than in CPVT1e and comparable to that in WT at baseline and with isoproterenol stimulation (Figure 6A and 6B). In contrast, the incidence of these events was similar in CPVT1e-S2808A and CPVT1e iPSC-CMs (Figure 6A and 6B), consistent with the ineffectiveness of pharmacological PKA inhibition (Figure 5B). Similar results were obtained from spontaneously beating cell clusters (Figure 6C and 6D). These data indicate that CaMKII phosphorylation of RYR2-S2814 is required to unmask the latent arrhythmic potential of the CPVT R46511 mutation.

We modeled the effect of ablation of the RYR2-S2814 CaMKII phosphorylation site on the development of reentry in CPVT engineered heart tissue. We fabricated opto-MTFs from CPVT1e-S2814A iPSC-CMs (Figure 6E). Unlike CPVT1p and CPVT1e tissues, rapid pacing and isoproterenol did not induce reentry in

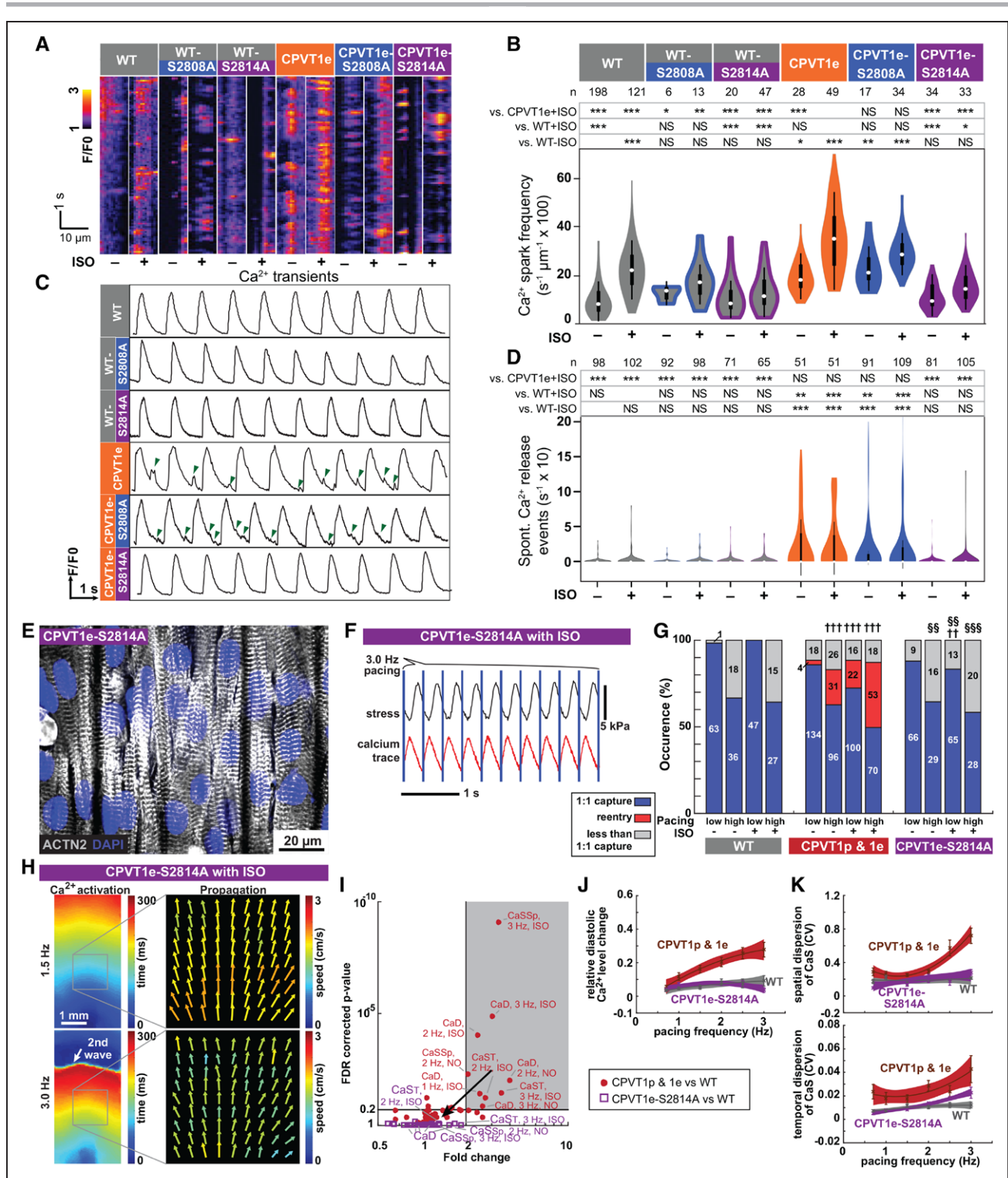


Figure 6. Ca²⁺-calmodulin-dependent protein kinase II (CaMKII) phosphorylation of ryanodine receptor (RyR2)-serine 2814 (S2814) is required to unmask the catecholaminergic polymorphic ventricular tachycardia (CPVT) arrhythmic phenotype. **A** and **B**, Incidence of Ca²⁺ sparks in quiescent induced pluripotent stem cell-derived cardiomyocytes (iPSC-CMs) in cell clusters. **A**, Representative traces. **B**, Quantitative analysis. Wild-type (WT) and CPVT1e data are the same as in Figure 5B. Steel-Dwass nonparametric test with multiple testing correction. **P*<0.05. ***P*<0.01. ****P*<0.001. **C** and **D**, Incidence of spontaneous Ca²⁺ release events in spontaneously beating iPSC-CMs in cell clusters. **C**, Representative traces. Green arrowheads indicate spontaneous Ca²⁺ release events. **D**, Quantitative analysis. WT and CPVT1e data are the same as in Figure 1D. Statistics and symbols as in **B**. **E**, Confocal image of opto-muscular thin film (opto-MTF) constructed with CPVT1e-S2814A iPSC-CMs. Myocytes are aligned by micromolded gelatin substrate. **F**, Representative CPVT1e-S2814A opto-MTF. Ca²⁺ transients and systolic contraction were coupled 1:1 with 3-Hz optical stimuli (blue lines). **G**, Occurrence of reentry in CPVT1e-S2814A compared with WT (††, †††) and CPVT1e (§§, §§§) opto-MTFs under matching conditions with the Pearson χ^2 test. The Bonferroni correction for multiple comparisons was applied for 3 possible pairwise tests performed with a corrected *P* threshold ††§§*P*<0.01/3. †††§§§*P*<0.001/3. Bars are labeled with sample numbers. **H**, Spatial maps of the same CPVT1e-S2814A opto-MTF paced at 1.5 or 3.0 Hz in the presence of isoproterenol (ISO). (Continued)

Figure 6 Continued. Ca^{2+} activation time and Ca^{2+} wave propagation speed were well organized and relatively homogeneous compared with CPVT1 (see Figure 3). **I**, Volcano plot of 60 tissue-level parameters of Ca^{2+} wave propagation (see Figure 3). Unlike CPVT1 tissue parameters, CPVT1e-S2814A tissue parameters were not statistically different from those of WT. **J** and **K**, Relative diastolic Ca^{2+} level change from basal condition (**J**), and spatial and temporal dispersion of Ca^{2+} wave propagation speed (**K**) as a function of pacing frequency under ISO stimulation in CPVT1e-S2814A compared with CPVT and WT. Smooth lines are quadratic functions fitted to the data; shaded areas and error bars show the 95% CI for the fit and SEM, respectively. Only tissues responding 1:1 to every stimulus were included in **I** to **K** ($n=12$ WT, 33 CPVT1p, 13 CPVT1e, 15 CPVT2e, and 18 CPVT1e-S2814A from >3 harvests). FDR indicates false discovery rate; and NS, not significant.

CPVT1e-S2814A tissues (Figure 6F and 6G and [Movie XVIII in the online-only Data Supplement](#)). These tissues retained well-ordered Ca^{2+} waves without regions of conduction block (Figure 6H), which we observed in CPVT1p, CPVT1e, and CPVT2e opto-MTFs under the same conditions (Figures 3 and 4). We analyzed Ca^{2+} wave propagation and other tissue properties of opto-MTFs between CPVT1e-S2814A and WT (purple, Figure 6I) and compared results with the previous analysis of the differences between CPVT and WT (Figure 3G, shown in red in Figure 6I). The RYR2-S2814A substitution did not alter global CaS (Figure XV in the [online-only Data Supplement](#)), but notably, it normalized the 3 parameters (relative diastolic Ca^{2+} level change from basal condition, spatial dispersion of CaS, and temporal dispersion of CaS) that were significantly different between CPVT and WT under higher pacing rates and isoproterenol. These 3 parameters became progressively higher in isoproterenol-treated CPVT than WT tissues with increasing pacing rate (Figure 3H and 3I and [Figure XV in the online-only Data Supplement](#)), but these abnormalities were abolished by the RYR2-S2814A substitution (Figure 6J and 6K and [Figure XV in the online-only Data Supplement](#)). These data show that preventing RYR2-S2814 phosphorylation normalizes pacing- and isoproterenol-induced CaS heterogeneity and relative diastolic Ca^{2+} level, resulting in a substrate that is less vulnerable to tissue-level reentry.

DISCUSSION

By integrating optogenetics, tissue engineering, lab-on-a-chip technology, and iPSC technology, we have created an engineered human tissue model to study arrhythmia mechanisms and to test antiarrhythmic therapy. We combined this platform with patient-derived and genome-edited iPSC-CMs to model the inherited arrhythmia CPVT at the tissue level. Similar strategies could be used to model other forms of inherited arrhythmia or to develop high-fidelity tissue-level models for cardiovascular drug toxicity studies.

Our engineered tissue model recapitulated key features of the clinical phenotype. First, under baseline conditions, the CPVT engineered tissues did not exhibit ectopic Ca^{2+} wave initiation, consistent with the normal baseline ECGs typically observed in patients at rest. This contrasts to the abnormal phenotype of unstimulated CPVT iPSC-CMs or dissociated murine CMs.³⁹ Second, adrenergic stimulation and rapid pacing induced reentrant rhythms in the CPVT engineered tissues, mimick-

ing exercise-induced ventricular tachycardia, which is a hallmark of the clinical phenotype.

Our CPVT models provide insights into disease pathogenesis. Although it was previously known that adrenergic stimulation of CaMKII was important for arrhythmogenesis in CPVT,^{4,5} our study identified a single CaMKII target site that must be phosphorylated to unmask the latent arrhythmic potential of the RYR2-R4651I CPVT mutation. This CaMKII target site is on RYR2 itself, at S2814. Phosphorylation of this site is known to increase RYR2 Ca^{2+} release and susceptibility to arrhythmia.^{35,36} Our results provide a molecular pathway that explains how exercise provokes arrhythmia in patients with CPVT and suggest that inhibiting this pathway will protect patients from developing lethal arrhythmia. We demonstrated that CaMKII activity is required to unmask the abnormal phenotype of several independent CPVT-causing RYR2 mutations (see the accompanying study by Bezzerides et al⁴⁰), although further work is required to demonstrate the precise requirement for RYR2-S2814 phosphorylation across multiple genotypes. The accompanying study by Bezzerides et al⁴⁰ further demonstrates that CaMKII inhibition by cardiac targeted gene therapy effectively suppresses ventricular arrhythmia in a CPVT mouse model. Together, these studies suggest that CaMKII inhibition may be a translatable therapy for CPVT.

The CPVT engineered heart tissue model provided insights into mechanisms by which RYR2 mutation may cause arrhythmia at the tissue level. In isolated cell clusters, CPVT mutations are well established to cause aberrant Ca^{2+} release from the sarcoplasmic reticulum.^{5,10-13} The resulting elevation of cytosolic Ca^{2+} drives depolarizing $\text{Na}^+-\text{Ca}^{2+}$ exchange through the sodium-calcium exchanger, resulting in afterdepolarizations that can trigger subsequent action potentials.¹ In an ex vivo study of a mouse model of CPVT, triggered activity originating from His-Purkinje cells was reported to be the source of ventricular tachycardia, setting up reentry and mediating the transition from polymorphic ventricular tachycardia to ventricular fibrillation.⁶ However, triggered activity in His-Purkinje cells alone is not sufficient for ventricular arrhythmia; a recent study demonstrated that the CPVT-inducing mutation must be present in working myocardium in addition to His-Purkinje to yield ventricular arrhythmia.⁸ In the working myocardium, the 2 conditions necessary for focal activity to occur are unlikely to be fulfilled. First, the intracellular Ca^{2+} waves associated with increased diastolic Ca^{2+} and Ca^{2+} release events rarely cross cell borders²⁴

and therefore do not form delayed afterdepolarizations synchronized among the quantity of cells necessary to elicit a triggered action potential. Second, electrotonic interaction between potential foci and neighboring tissue (so-called source-to-load mismatch) is expected, in contrast to observations made in single cells or clusters of few cells, to dampen the amount of local depolarization and to counteract or prevent ectopic action potential formation.⁴¹ Likely for these same reasons, simulated exercise did not stimulate ectopic impulse initiation in our engineered CPVT tissues. Rather, a high pacing rate and isoproterenol stimulation markedly increased heterogeneity of Ca²⁺ wave propagation and elevated diastolic Ca²⁺ in CPVT tissue, resulting in local depolarization, propagation block, and subsequent reentry. This is consistent with computational modeling studies in which subthreshold afterdepolarizations increased repolarization heterogeneity and locally impaired cardiomyocyte excitability.³⁰ Thus, our data based on Ca²⁺ measurements, in combination with computational electric modeling and mouse models, suggest that CPVT mutations cause heterogeneity of action potential repolarization and excitability, creating a vulnerable substrate within working myocardium that sustains reentrant arrhythmias. Although reentrant spiral waves were initiated by collision of optically stimulated propagating Ca²⁺ transients with regions of focal conduction block in our experiments, triggered activity arising within the His-Purkinje system is likely to play a role as an initiating mechanism in whole hearts. Further studies in animal models are required to test this hypothesis.

Conclusions

We developed a human engineered tissue platform to elucidate the pathogenesis of inherited arrhythmias, and we used this platform to gain molecular and pathophysiological insights into CPVT. It is important to point out important limitations of the current engineered tissue model. One limitation is that we were unable to measure membrane voltage because currently available optical voltage sensors have greater toxicity, inadequate signal-to-noise properties, or spectral incompatibility with our optical actuator. Improved optical voltage sensors or refinements to the patterned substrate that permit multielectrode array recordings will allow measurement of membrane voltage or extracellular electrograms and provide additional insights into the mechanisms responsible for reentry. A second limitation is that current stem cell-derived cardiomyocytes are immature compared with adult cardiomyocytes,⁴² and consequently, findings made in iPSC-CM systems such as dynamic conduction block precipitating reentry require further validation in animal models and in patients. Ongoing efforts to improve iPSC-CM maturity, combined with continued development of physiological, tissue-

level arrhythmia assays, will further advance our ability to model human arrhythmias in *in vitro* systems. Finally, the molecular and cellular mechanisms that lead to heterogeneous calcium transient propagation and dynamic conduction block in CPVT opto-MTFs stimulated with isoproterenol and rapid pacing are unclear. Addressing these questions will be fertile ground for future studies.

ARTICLE INFORMATION

Received January 14, 2019; accepted May 30, 2019.

The online-only Data Supplement is available with this article at <https://www.ahajournals.org/doi/suppl/10.1161/CIRCULATIONAHA.119.039711>.

Correspondence

Kevin Kit Parker, PhD, 29 Oxford Street, Pierce Hall, Cambridge, MA 02130; or William T. Pu, MD, 300 Longwood Ave, Boston, MA 02115. Email kkparker@seas.harvard.edu or wpu@pulab.org

Affiliations

Disease Biophysics Group, Wyss Institute for Biologically Inspired Engineering, John A. Paulson School of Engineering and Applied Sciences (S.-J.P., K.Y.L., S.L.K., F.S.P., P.H.C., K.K.P.), and Harvard Stem Cell Institute (W.T.P., K.K.P.), Harvard University, Cambridge, MA. State Key Laboratory of Biocatalysis and Enzyme Engineering, School of Life Science, Hubei University, Wuhan, China (D.Z., Y.Q., P.Y., S.X.). Department of Cardiology, Boston Children's Hospital, MA (D.Z., Y.L., V.J.B., X.L., F.L., J.G., A.E.R., D.J.A., W.T.P., K.K.P.). Department of Pediatrics, West China Second University Hospital, Sichuan University, Chengdu (Y.L.). Department of Pathology, Beth Israel Deaconess Medical Center and Harvard Medical School, Boston, MA (A.G.K.). Sogang-Harvard Research Center for Disease Biophysics, Sogang University, Seoul, South Korea (K.K.P.). Dr Park is currently at the Coulter Department of Biomedical Engineering, Georgia Institute of Technology, and Emory University School of Medicine, Atlanta.

Acknowledgments

D.Z. and S.-J.P. contributed equally to this study; their authorship order is interchangeable, and they are listed in alphabetical order. D.Z. and S.-J.P. designed and performed experiments, analyzed data, organized figures, and wrote the paper. D.Z. developed the patient-derived and genome-edited iPSC-CMs and performed cell cluster assays, with help from Y.Q., P.Y., S.X., X.L., and F.L. S.-J.P. developed the opto-MTF platform and analysis methods, performed experiments on opto-MTFs, and analyzed data. Y.L. performed the Western blot experiments. J.G. and A.E.R. recruited the patient with CPVT. V.J.B. contributed to iPSC-CM characterization and with D.J.A. provided clinical data and insights. K.Y.L. conducted immunostaining. S.L.K. assisted with opto-MTF fabrication and analysis. K.Y.L. and F.S.P. optimized gelatin substrates and provided insights in experimental design and analysis. P.H.C. performed NRVM harvest for MTF optimization. A.G.K. provided mechanistic insights and edited the manuscript. W.T.P. conceived of and organized the project and cowrote the manuscript. K.K.P. supervised the project, developed the opto-MTF platform, and edited the manuscript.

Sources of Funding

Dr Pu was funded by National Institutes of Health grant U01 HL100401, the Boston Children's Translational Investigator Service, and the Boston Children's Heart Center. The Boston Children's Hospital Inherited Cardiac Arrhythmia Program (Drs Abrams and Pu) is funded by generous support from the Mannion and Roberts families. Dr Parker was funded by the John A. Paulson School of Engineering and Applied Sciences at Harvard, the Wyss Institute for Biologically Inspired Engineering at Harvard, National Institutes of Health National Center for Advancing Translational Sciences grant UH3TR000522, and National Science Foundation Materials Research Science and Engineering Center grant DMR-1420570. Drs Parker and Pu were sponsored by National Institutes of Health National Center for Advancing Translational Sciences grant 1-UG3-HL-141798-01. Drs Parker, Pu, and Abrams were supported by a collaborative research grant from the American Heart Association (16CSA28750006). Dr Zhang was funded by the Ministry of Science and Technology of China (National Science and Technology Major Project, grant 2018YFA0109100)

and the National Natural Science Foundation of China (grants 31871496 and 31741090). The views and conclusions contained in this document are those of the authors and should not be interpreted as representing the official policies, either expressed or implied, of the National Institutes of Health, the Defense Advanced Research Projects Agency, the US Government, or the Chinese. This work was performed in part at the Center for Nanoscale Systems, a member of the National Nanotechnology Infrastructure Network, which is supported by the National Science Foundation under award ECS-0335765. The Center for Nanoscale Systems is part of Harvard University. Certain aspects of the article are described in US patents 8,492,150 and 9,669,141 and US patent cooperation treaty PCT/US2015/051818.

Disclosures

None.

REFERENCES

- Venetucci L, Denegri M, Napolitano C, Priori SG. Inherited calcium channelopathies in the pathophysiology of arrhythmias. *Nat Rev Cardiol*. 2012;9:561–575. doi: 10.1038/nrcardio.2012.93
- Peng W, Shen H, Wu J, Guo W, Pan X, Wang R, Chen SRW, Yan N. Structural basis for the gating mechanism of the type 2 ryanodine receptor RyR2. *Science*. 2016;354:AAH5324.
- Priori SG, Chen SR. Inherited dysfunction of sarcoplasmic reticulum Ca²⁺ handling and arrhythmogenesis. *Circ Res*. 2011;108:871–883. doi: 10.1161/CIRCRESAHA.110.226845
- Liu N, Ruan Y, Denegri M, Bachetti T, Li Y, Colombi B, Napolitano C, Coetzee WA, Priori SG. Calmodulin kinase II inhibition prevents arrhythmias in RyR2(R4496C+/-) mice with catecholaminergic polymorphic ventricular tachycardia. *J Mol Cell Cardiol*. 2011;50:214–222. doi: 10.1016/j.yjmcc.2010.10.001
- Di Pasquale E, Lodola F, Miragoli M, Denegri M, Avelino-Cruz JE, Buonocore M, Nakahama H, Portararo P, Bloise R, Napolitano C, Condorelli G, Priori SG. CaMKII inhibition rectifies arrhythmic phenotype in a patient-specific model of catecholaminergic polymorphic ventricular tachycardia. *Cell Death Dis*. 2013;4:e843. doi: 10.1038/cddis.2013.369
- Cerrone M, Noujaim SF, Tolkacheva EG, Talkachou A, O'Connell R, Berenfeld O, Anumonwo J, Pandit SV, Vikstrom K, Napolitano C, Priori SG, Jalife J. Arrhythmogenic mechanisms in a mouse model of catecholaminergic polymorphic ventricular tachycardia. *Circ Res*. 2007;101:1039–1048. doi: 10.1161/CIRCRESAHA.107.148064
- Bers DM. Calcium cycling and signaling in cardiac myocytes. *Annu Rev Physiol*. 2008;70:23–49. doi: 10.1146/annurev.physiol.70.113006.100455
- Flores DJ, Duong T, Brandenberger LO, Mitra A, Shirali A, Johnson JC, Springer D, Noguchi A, Yu ZX, Ebert SN, Ludwig A, Knollmann BC, Levin MD, Pfeifer K. Conditional ablation and conditional rescue models for Casq2 elucidate the role of development and of cell-type specific expression of Casq2 in the CPVT2 phenotype. *Hum Mol Genet*. 2018;27:1533–1544. doi: 10.1093/hmg/ddy060
- Bezzarides VJ, Zhang D, Pu WT. Modeling inherited arrhythmia disorders using induced pluripotent stem cell-derived cardiomyocytes. *Circ J*. 2016;81:12–21. doi: 10.1253/circj.CJ-16-1113
- Jung CB, Moretti A, Mederos y Schnitzler M, Iop L, Storch U, Bellin M, Dorn T, Ruppenthal S, Pfeiffer S, Goedel A, Dirschinger RJ, Seyfarth M, Lam JT, Sinnecker D, Gudermann T, Lipp P, Laugwitz KL. Dantrolene rescues arrhythmogenic RYR2 defect in a patient-specific stem cell model of catecholaminergic polymorphic ventricular tachycardia. *EMBO Mol Med*. 2012;4:180–191. doi: 10.1002/emmm.201100194
- Preininger MK, Jha R, Maxwell JT, Wu Q, Singh M, Wang B, Dalal A, Mceachin ZT, Rossoll W, Hales CM, Fischbach PS, Wagner MB, Xu C. A human pluripotent stem cell model of catecholaminergic polymorphic ventricular tachycardia recapitulates patient-specific drug responses. *Dis Model Mech*. 2016;9:927–939. doi: 10.1242/dmm.026823
- Fatima A, Xu G, Shao K, Papadopoulos S, Lehmann M, Arnáiz-Cot JJ, Rosa AO, Nguemo F, Matzkies M, Dittmann S, Stone SL, Linke M, Zechner U, Beyer V, Hennies HC, Rosenkranz S, Klauke B, Parwani AS, Haverkamp W, Pfitzer G, Farr M, Cleemann L, Morad M, Miltung H, Hescheler J, Saric T. In vitro modeling of ryanodine receptor 2 dysfunction using human induced pluripotent stem cells. *Cell Physiol Biochem*. 2011;28:579–592. doi: 10.1159/000335753
- Itzhaki I, Maizels L, Huber I, Gepstein A, Arbel G, Caspi O, Miller L, Belhassen B, Nof E, Glikson M, Gepstein L. Modeling of catecholaminergic polymorphic ventricular tachycardia with patient-specific human-induced pluripotent stem cells. *J Am Coll Cardiol*. 2012;60:990–1000. doi: 10.1016/j.jacc.2012.02.066
- Qu Z, Weiss JN. Mechanisms of ventricular arrhythmias: from molecular fluctuations to electrical turbulence. *Annu Rev Physiol*. 2015;77:29–55. doi: 10.1146/annurev-physiol-021014-071622
- Feinberg AW, Feigel A, Shevkopyas SS, Sheehy S, Whitesides GM, Parker KK. Muscular thin films for building actuators and powering devices. *Science*. 2007;317:1366–1370. doi: 10.1126/science.1146885
- Wang G, McCain ML, Yang L, He A, Pasqualini FS, Agarwal A, Yuan H, Jiang D, Zhang D, Zangi L, Geva J, Roberts AE, Ma Q, Ding J, Chen J, Wang DZ, Li K, Wang J, Wanders RJ, Kulik W, Vaz FM, Laflamme MA, Murry CE, Chien KR, Kelley RI, Church GM, Parker KK, Pu WT. Modeling the mitochondrial cardiomyopathy of Barth syndrome with induced pluripotent stem cell and heart-on-chip technologies. *Nat Med*. 2014;20:616–623. doi: 10.1038/nm.3545
- McCain ML, Agarwal A, Nesmith HW, Nesmith AP, Parker KK. Micro-molded gelatin hydrogels for extended culture of engineered cardiac tissues. *Biomaterials*. 2014;35:5462–5471. doi: 10.1016/j.biomaterials.2014.03.052
- Weinberger F, Mannhardt I, Eschenhagen T. Engineering cardiac muscle tissue: a maturing field of research. *Circ Res*. 2017;120:1487–1500. doi: 10.1161/CIRCRESAHA.117.310738
- Wang G, Yang L, Grishin D, Rios X, Ye LY, Hu Y, Li K, Zhang D, Church GM, Pu WT. Efficient, footprint-free human iPSC genome editing by consolidation of Cas9/CRISPR and piggyBac technologies. *Nat Protoc*. 2017;12:88–103. doi: 10.1038/nprot.2016.152
- Ran FA, Hsu PD, Wright J, Agarwala V, Scott DA, Zhang F. Genome engineering using the CRISPR-Cas9 system. *Nat Protoc*. 2013;8:2281–2308. doi: 10.1038/nprot.2013.143
- Park SJ, Gazzola M, Park KS, Park S, Di Santo V, Blevins EL, Lind JU, Campbell PH, Dauth S, Capulli AK, Pasqualini FS, Ahn S, Cho A, Yuan H, Maoz BM, Vijaykumar R, Choi JW, Deisseroth K, Lauder GV, Mahadevan L, Parker KK. Phototactic guidance of a tissue-engineered soft-robotic ray. *Science*. 2016;353:158–162. doi: 10.1126/science.aaf4292
- Dittgen T, Nimmerjahn A, Komai S, Licznarski P, Waters J, Margrie TW, Helmchen F, Denk W, Brecht M, Osten P. Lentivirus-based genetic manipulations of cortical neurons and their optical and electrophysiological monitoring in vivo. *Proc Natl Acad Sci USA*. 2004;101:18206–18211. doi: 10.1073/pnas.0407976101
- Benjamini Y, Hochberg Y. Controlling the false discovery rate: a practical and powerful approach to multiple testing. *J R Stat Soc Series B Stat Methodol*. 1995;57:289–300.
- Baader AP, Büchler L, Bircher-Lehmann L, Kléber AG. Real time, confocal imaging of Ca(2+) waves in arterially perfused rat hearts. *Cardiovasc Res*. 2002;53:105–115. doi: 10.1016/s0008-6363(01)00423-0
- Grosberg A, Alford PW, McCain ML, Parker KK. Ensembles of engineered cardiac tissues for physiological and pharmacological study: heart on a chip. *Lab Chip*. 2011;11:4165–4173. doi: 10.1039/c1lc20557a
- Li Q, Ni RR, Hong H, Goh KY, Rossi M, Fast VG, Zhou L. Electrophysiological properties and viability of neonatal rat ventricular myocyte cultures with inducible ChR2 expression. *Sci Rep*. 2017;7:1531. doi: 10.1038/s41598-017-01723-2
- Penttinen K, Swan H, Vanninen S, Paavola J, Lahtinen AM, Kontula K, Aalto-Setälä K. Antiarrhythmic effects of dantrolene in patients with catecholaminergic polymorphic ventricular tachycardia and replication of the responses using iPSC models. *PLoS One*. 2015;10:e0125366. doi: 10.1371/journal.pone.0125366
- Kobayashi S, Yano M, Uchinoumi H, Suetomi T, Susa T, Ono M, Xu X, Tateishi H, Oda T, Okuda S, Doi M, Yamamoto T, Matsuzaki M. Dantrolene, a therapeutic agent for malignant hyperthermia, inhibits catecholaminergic polymorphic ventricular tachycardia in a RyR2(R2474S/+) knock-in mouse model. *Circ J*. 2010;74:2579–2584.
- Peracchia C. Chemical gating of gap junction channels; roles of calcium, pH and calmodulin. *Biochim Biophys Acta*. 2004;1662:61–80. doi: 10.1016/j.bbame.2003.10.020
- Liu MB, de Lange E, Garfinkel A, Weiss JN, Qu Z. Delayed afterdepolarizations generate both triggers and a vulnerable substrate promoting reentry in cardiac tissue. *Heart Rhythm*. 2015;12:2115–2124. doi: 10.1016/j.hrthm.2015.06.019
- Glass DB, Cheng HC, Mende-Mueller L, Reed J, Walsh DA. Primary structural determinants essential for potent inhibition of cAMP-dependent protein kinase by inhibitory peptides corresponding to the active portion of the heat-stable inhibitor protein. *J Biol Chem*. 1989;264:8802–8810.

32. Ji Y, Li B, Reed TD, Lorenz JN, Kaetzel MA, Dedman JR. Targeted inhibition of Ca²⁺/calmodulin-dependent protein kinase II in cardiac longitudinal sarcoplasmic reticulum results in decreased phospholamban phosphorylation at threonine 17. *J Biol Chem*. 2003;278:25063–25071. doi: 10.1074/jbc.M302193200
33. Pereira L, Cheng H, Lao DH, Na L, van Oort RJ, Brown JH, Wehrens XH, Chen J, Bers DM. Epac2 mediates cardiac β 1-adrenergic-dependent sarcoplasmic reticulum Ca²⁺ leak and arrhythmia. *Circulation*. 2013;127:913–922. doi: 10.1161/CIRCULATIONAHA.12.148619
34. Anderson ME, Brown JH, Bers DM. CaMKII in myocardial hypertrophy and heart failure. *J Mol Cell Cardiol*. 2011;51:468–473. doi: 10.1016/j.yjmcc.2011.01.012
35. Wehrens XH, Lehnart SE, Reiken SR, Marks AR. Ca²⁺/calmodulin-dependent protein kinase II phosphorylation regulates the cardiac ryanodine receptor. *Circ Res*. 2004;94:e61–e70. doi: 10.1161/01.RES.0000125626.33738.E2
36. van Oort RJ, McCauley MD, Dixit SS, Pereira L, Yang Y, Respress JL, Wang Q, De Almeida AC, Skapura DG, Anderson ME, Bers DM, Wehrens XH. Ryanodine receptor phosphorylation by calcium/calmodulin-dependent protein kinase II promotes life-threatening ventricular arrhythmias in mice with heart failure. *Circulation*. 2010;122:2669–2679. doi: 10.1161/CIRCULATIONAHA.110.982298
37. Wehrens XH, Lehnart SE, Reiken S, Vest JA, Wronska A, Marks AR. Ryanodine receptor/calcium release channel PKA phosphorylation: a critical mediator of heart failure progression. *Proc Natl Acad Sci USA*. 2006;103:511–518. doi: 10.1073/pnas.0510113103
38. Shan J, Betzenhauser MJ, Kushnir A, Reiken S, Meli AC, Wronska A, Dura M, Chen BX, Marks AR. Role of chronic ryanodine receptor phosphorylation in heart failure and β -adrenergic receptor blockade in mice. *J Clin Invest*. 2010;120:4375–4387. doi: 10.1172/JCI37649
39. Sedej S, Heinzel FR, Walther S, Dybkova N, Wakula P, Groborz J, Gronau P, Maier LS, Vos MA, Lai FA, Napolitano C, Priori SG, Kocksämper J, Pieske B. Na⁺-dependent SR Ca²⁺ overload induces arrhythmogenic events in mouse cardiomyocytes with a human CPVT mutation. *Cardiovasc Res*. 2010;87:50–59. doi: 10.1093/cvr/cvq007
40. Bezzerides VJ, Caballero A, Wang S, et al. Gene therapy for catecholaminergic polymorphic ventricular tachycardia by inhibition of Ca²⁺/calmodulin-dependent kinase II. *Circulation*. 2019; in press. doi: 10.1161/CIRCULATIONAHA.118.038514
41. Zaglia T, Pianca N, Borile G, Da Broi F, Richter C, Campione M, Lehnart SE, Luther S, Corrado D, Miquelol L, Mongillo M. Optogenetic determination of the myocardial requirements for extrasystoles by cell type-specific targeting of ChannelRhodopsin-2. *Proc Natl Acad Sci USA*. 2015;112:E4495–E4504. doi: 10.1073/pnas.1509380112
42. Yang X, Pabon L, Murry CE. Engineering adolescence: maturation of human pluripotent stem cell-derived cardiomyocytes. *Circ Res*. 2014;114:511–523. doi: 10.1161/CIRCRESAHA.114.300558